EUROPHYSICS LETTERS 15 February 1999

Europhys. Lett., **45** (4), pp. 526-532 (1999)

Phase segregation in polymer thin films: Elucidations by X-ray and scanning force microscopy

H. ADE[1](*), D. A. WINESETT[1], A. P. SMITH[2], S. QU[3], S. GE[3], J. SOKOLOV[3] and M. RAFAILOVICH[3]

[1] *Department of Physics, North Carolina State University Raleigh, NC 27695-8202, USA*
[2] *Department of Materials Science and Engineering North Carolina State University - Raleigh, NC 27695-8202, USA*
[3] *Department of Materials Science and Engineering SUNY@Stony Brook, Stony Brook, NY11794, USA*

(received 15 July 1998; accepted in final form 8 December 1998)

PACS. 83.10Nn – Polymer dynamics.
PACS. 83.80Es – Polymer blends.
PACS. 61.10Ht – X-ray absorption spectroscopy: EXAFS, NEXAFS, XANES, etc.

Abstract. – We have used quantitative X-ray microscopy in combination with Scanning Force Microscopy to monitor the phase separation of spun cast thin films of polystyrene and poly(methyl methacrylate) blends upon annealing. Both techniques complement and enhance each other in elucidating the complicated structures that develop as a function of annealing time. We have determined the composition of the mixed phases that result from solvent spin casting. We subsequently observe the sudden rearrangement into domains much smaller than those originally formed. Unique, intricate hydrodynamic mass flow patterns form during coarsening which are in qualitative agreement with recent simulations of phase segregation in two-dimensional viscous fluids. Complicated polymer-polymer interfaces persist even in the later stages that are explained in terms of the geometric constraints of a thin film and the dependance of polymer viscosity on film thickness.

Thin film polymer blends have considerable technological importance and are used in numerous applications ranging from multi-color photographic printing to paints, adhesives and protective coatings. Compared to the bulk properties, less is known about the properties of blends when they are processed into thin films. Numerous studies [1-10] have shown that for binary polymer blends the spinodal decomposition and coarsening process can be more complex in thin films where various boundary conditions are imposed. Most of the recent studies of phase separation in thin films relied on various scanning force and optical microscopy methods. These methods can only probe features that vary in topography, mechanical properties or have large differences in reflectivity, and hence these studies have mostly concentrated on

(*) E-mail: Harald_ade@ncsu.edu

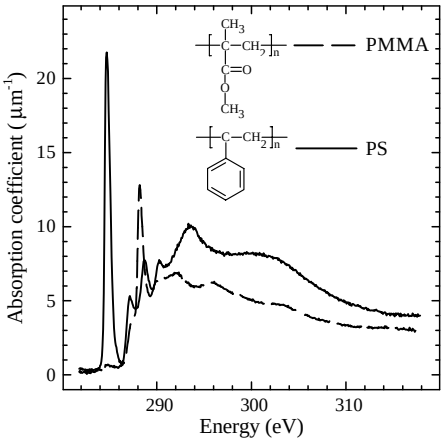

Fig. 1. – Reference spectra of PS and PMMA normalized to the pre- and post-edge linear absorption coefficients of Henke [11], assuming a density of 1.07 g/cm^3 for PS and 1.19 g/cm^3 for PMMA [12].

the growth of large domains in the very late stages of phase separation [4, 6-10]. While growing domain sizes can be observed, the determination of the local composition within domains is elusive and these techniques are unable to unambiguously resolve the mass flow. Consequently, while a variety of morphologies that evolve during the phase separation process in polymer thin films have been observed [3-9], the composition of two- and three-dimensional morphologies and its time-dependent evolution has never been directly determined in the early stages of phase separation. In this report, we present the results of combining quantitative Near Edge X-ray Absorption Fine Structure (NEXAFS) microscopy with Scanning Force Microscopy (SFM) to observe and characterize the phase separation and coarsening in a thin film (146 nm) over a wide range of time scales. The model polymer blend utilized consisted of monodisperse (Molecular weight Mw = 27000, Mw/Mn $<$ 1.05) polystyrene (PS) and poly(methyl methacrylate) (PMMA) (Mw = 27000, Mw/Mn $<$ 1.1). We have determined the composition of the phases in the as-spun films, observed the phase separation into smaller domains, and the development of ragged domains during the early stages of coarsening. Our observations of the early stages are particularly interesting because recent lattice Boltzmann simulations by Wagner and Yeomans [13] on thin layers of binary fluids indicate that the early stages of the spinodal decomposition process are even more sensitive to the dimensionality of the film than the later stages [14]. These results predict that the dominant growth mechanism in thin films depends on the competition between the relative viscosities, the diffusivities of the two liquids, as well as the amplitude of the surface capillary waves relative to the domain size. In contrast to bulk spinodal decomposition, the resulting patterns are predicted to lack scale invariance and to develop with time-dependent rate laws. Depending on the viscosities, different morphologies, including ragged ones, can evolve. Our observations of the various time domains and the formation of a ragged morphology are in qualitative agreement with Wagner and Yeomans.

Thin films composed of 50/50 weight percent PS/PMMA blends were spun cast out of toluene solution onto Si substrates with a native oxide layer. The thickness of the films, 143 nm, was determined by multiple wavelength ellipsometry. The films were annealed for varying times and sections were subsequently transferred to carbon-coated TEM grids for investigation with the Stony Brook Scanning Transmission X-ray Microscope (STXM) [15-17] at the National Synchrotron Light Source. We acquired NEXAFS images of the thin films at

photon energies that included characteristic peaks of the component polymers (see fig. 1). To obtain the composition profiles from the transmission images we utilized the "single-value decomposition" procedure described in ref. [18]. This procedure uses the carefully measured absorption coefficients from the reference homopolymers (fig. 1). We determined mass thickness maps of each constituent polymer, and compared the summed maps (total thickness) to SFM topographs. The individual NEXAFS compositional maps were compared to friction and lateral force measurements using a SFM with an externally driven amplitude modulation. Due to the slight difference in surface friction and modulus, these techniques can be used to differentiate between PS and PMMA phases [9, 19]. The surface composition and interface morphology of the PMMA phase was also checked and compared to NEXAFS microscopy by washing off the PS layer in cyclohexane, a selective solvent for PS.

From the quantitative NEXAFS maps (fig. 2) we can see directly that the unannealed, solution cast blend (fig. 2A-C) is already phase separated into small PS-rich regions and a continuous PMMA-rich phase. We observed significant amounts of PS in a cyclohexane washed unannealed sample with quantitative NEXAFS maps and sample averaged NEXAFS spectroscopy (not shown here). Combining the results from the washed and unwashed sample, we find that the two polymers are partially mixed with the PMMA/PS concentration ratios varying from about 80/20% in the continuous PMMA-rich matrix to about 20/80% in the PS-rich islands. The NEXAFS maps also indicate a gradient layer between these domains as well as a thin PMMA layer near the substrate. Since the polymers are immiscible in the melt, the initial, mixed compositions observed are a result of co-dissolution in toluene during the solvent casting process. From figs. 2D-F, we see that immediately upon annealing, in the absence of solvent, drastic reorganization occurs. It is interesting to note that the large round PS domains that form after annealing for one week (figs. 2P-R) are not simply a result of the gradual coalescence of the small, PS-rich domains, which are observed prior to annealing. Rather, the mixed PS/PMMA domains phase separate into smaller domains and form intricate coarsening patterns for pure components (figs. 2D-L) similar to the ones predicted in ref. [13]. The initial changes in the first few minutes are the most rapid (note the change in scale between figs. 2A-F and G-L). This is qualitatively consistent with the results of ref. [13] which show a rapid initial growth of patterns in the hydrodynamic flow regime. In addition, the jagged flow patterns and rough interfaces in images 2D-K are similar to the patterns exhibited in these simulations and occur when the wavelength of capillary waves is about the same as the domain size [20]. Once the domains are circular, coalescence occurs through much slower diffusion/collision processes. This change in growth exponent, which is a function of the patterns formed, leads to the predicted lack of scale invariance. From the STXM figures, one can see additional features that are similar to those obtained in the simulations. For example, we see the scale-dependent crossover from hydrodynamic flow to diffusion/collision in figs. 2 E, H, F and K where large, interconnected domains with rough interfaces coexist with smaller, circular domains. Since these circular domains can only grow via collisions with each other, they remain trapped for long times within a matrix of the opposite phase. Since the ratio between the relative viscosities and diffusion coefficients of the two components was shown to determine the crossover between viscous flow and diffusion limited regimes, we must first know these parameters before we can compare time scales quantitatively with the theoretical model in ref. [13]. Previous work demonstrated that the diffusion coefficient of PS is a strong function of the film thickness or distance from the silicon interface [21]. Preliminary results show that a similar dependence may exist for PMMA [22]. Consequently, the ratio of the diffusivities is changing as the three-dimensional morphology develops. This effect may also contribute to the lack of scale invariance and explains the decrease in the dynamics observed with increasing annealing time. The PMMA mass thickness varies from 110 nm in the PMMA-rich regions

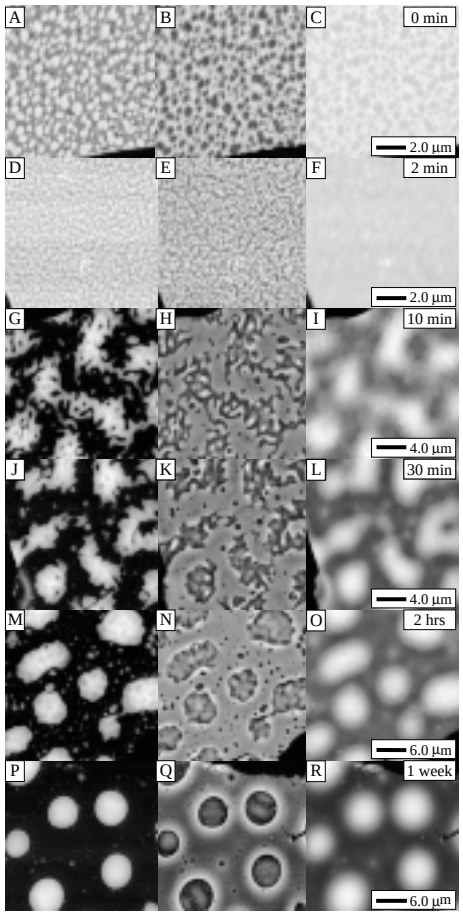

Fig. 2. – PS mass thickness (left column), PMMA mass thickness (middle column) and total thickness maps (right column) of a nominally 143 nm thick 50/50 w/w% PS/PMMA blend annealed for (A-C) 0 min, (D-F) 2 min, (G-I) 10 min, (J-L) 30 min, (M-O) 2 hrs, and (P-R) 1 week. All images are individually scaled for good contrast, with Black = 0 and White = maximum thickness. The maximum thickness of the films increases from 145 nm in A, to 460 nm in R. The raw data comprised a set of four to six images for each sample area investigated, including energies corresponding to the C═C 1*s* to π^* transition at 285.2 eV of the aromatic group of PS, the PS-dominated σ^* peak at 295 eV, the C═O 1*s* to π^* transition of the carbonyl in the PMMA, and the pre and post edge images at 281 and 310 eV, respectively. Single-value decomposition using densities of 1.07 g/cm^3 for PS and 1.19 g/cm^3 for PMMA resulted in the quantitative composition maps.

of the unannealed sample (fig. 2B) to about 60 nm of pure PMMA in the continuous phase after one week of annealing. The PMMA underneath the PS domains is on average less than 20 nm thick and even thinner near the edge. The PS thickness increases to approximately 450 nm in the spherical regions from an average thickness of approximately 70 nm in the unannealed film. This thickness difference corresponds to a tenfold decrease in the diffusion coefficient of PMMA [22]. The corresponding increase in the PS diffusion coefficient only affects reorganization within the PS domains. Since PMMA forms the continuous phase in these samples, it determines the rate at which the isolated PS regimes can collide and coalesce. Experiments are currently in progress to measure the diffusion coefficient as a function of film

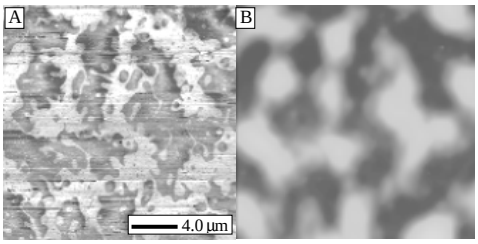

Fig. 3. – A Lateral force modulation and B topography maps of a sample annealed for 10 min.

thickness for PMMA. Coupled with the thickness maps shown in fig. 2, we will then be able to obtain quantitative comparisons with the theoretical models. Alternatively, films forced into a flat geometry between two surfaces would facilitate a quantitative comparison to theory.

In the PS/PMMA blend system, the two polymers can also be differentiated by the slight difference in their frictional coefficient and solubility in different organic solvents. One can therefore also study some of the surface and three-dimensional aspects of the PS/PMMA interface with SFM. The limitation of washing is that only relatively pure PS regions are dissolved [23] and that the PMMA remains in a distorted, swollen state. A comparison of the SFM data to the STXM results allows, however, for the identification of possible artifacts. The combination of the two methods showed indeed some additional aspects affecting the coarsening and coalescence process. Figure 3 shows a lateral force modulation scan and topograph [24] of the same sample imaged with STXM in figs. 2G-L. The low regions appear on average brighter (or have larger friction) than the taller regions. The intricate morphology visible in the friction image (fig. 3A) matches the compositional images derived from NEXAFS (fig. 2G). We can associate the bright and dark areas of fig. 3A with PMMA- and PS-rich regions, respectively, and can conclude that there are indeed two different surface phases that match the phases determined with STXM. Figure 4 shows the three-dimensional rendering of the topographical scans of samples annealed for 10 minutes and 65 hours and washed in cyclohexane to remove the PS phase. The remaining features are those of the pure PMMA phase. One can see that at early times PMMA "spikes" [25] attached to a PMMA sublayer are distributed throughout the sample. As annealing progresses (fig. 2Q and 4B), each PS droplet is surrounded by a wall of PMMA. Prior to the STXM experiments it was thought that the spikes within the walls of fig. 4B were impurities left behind by the solvent rinse. From figs. 2M-R it is clear that these are

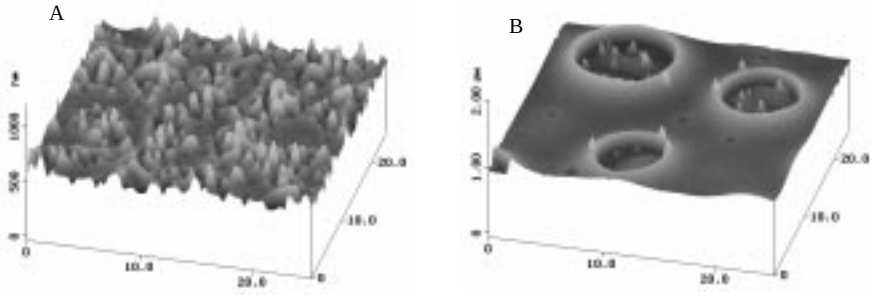

Fig. 4. – AFM topographs of samples with the surface PS removed with cyclohexane: after 10 min (A), and 64 h (B) of annealing.

some of the original spikes that formed at early times and were swept along with the receding PS phase [26]. Similar small and isolated PS domains (seen as holes in the matrix of fig. 4) are also present in the PMMA phase. The PS features can easily be explained by diffusion-limited trapping where coalescence in a hostile PMMA matrix is only possible by collision of the droplets [13]. The presence of the PMMA spikes inside the PS droplets is more perplexing. From the SFM data, it is clear that these droplets are in contact with the PMMA sublayer that is continuous throughout the samples. However, the spikes do not get absorbed within this sublayer. This may be a manifestation of a "two fluid" behavior [21] whereby diffusion of the spikes into the thin layer is significantly inhibited due to the strong interaction pinning of the PMMA chains in the thin layer to the Si substrate. PMMA domains become trapped between the PS domain and a high-viscosity PMMA sublayer, resulting in a quasi 2-dimensional system in analogy to the small PS domains trapped in the PMMA matrix. One should also note that the PMMA interface beneath the PS droplets has a long wavelength undulation not apparent on the PMMA surface in contact with vacuum (fig. 2Q). This undulation appears as thickness stripes in the PMMA map with an amplitude approximately 5-6 times larger than the RMS roughness of the surrounding PMMA matrix (figs. 2N and 2Q). Since the RMS amplitude A of capillary waves at an interface are also known to scale as $A \sim \gamma^{-1/2}$ or approximately 5 for this system [27] we believe that these features are caused by the resonant capillary modes excited in the confined area beneath the PS droplets. These are the capillary modes that were also invoked in ref. [13] and explain the rough features seen in the mostly 2-D patterns (figs. 2G-O) observed at the initial stages of the coarsening process.

In summary, we have obtained new information about the composition, morphology and dynamics during the phase separation process of thin films of PS/PMMA blends prepared by spin casting from toluene solution. We have monitored the phase separation process over a wide range of times and observed three stages: 1) initial phase separation of the mixed phases, 2) rapid coarsening and unique mass flow patterns that are very different from the coarsening of phase separation in 3-dimensional systems, and 3) coalescence similar to classic spinodal decomposition in the late stages but with persisting complicated 3-dimensional interfaces. In particular, we have observed the complex morphology during coarsening and the different scaling regimes recently predicted by Wagner and Yeomans [13]. During the late stages, we have observed PMMA spikes and capillary wave induced interface modulations below the PS domains. To characterize the complicated structures formed and their evolutions we have utilized quantitative compositional analysis based on NEXAFS microscopy in conjunction with AFM techniques. Both techniques complement and enhance each other. Our approach will be useful to study details about the dynamics of the phase separation process in a variety of thin polymer films.

***

NEXAFS data acquired with the Stony Brook STXM developed by the group of J. Kirz and C. Jacobsen at SUNY Stony Brook (DOE grant DE-FG02-89ER60858; NSF grant DBI-9605045). The zone plates were developed by S. Spector and C. Jacobsen of Stony Brook and D. Tennant of Lucent Technologies Bell Labs (NSF grant ECS-9510499). HA, DAW and APS are supported by an NSF Young Investigator Award (DMR-9458060). SQ SG, MR, JS at Stony Brook supported by NSF DMR-9732230 (MRSEC Program) and DOE-SG02-93-ER45481.

REFERENCES

[1] Reich S. and Cohen Y., *J. Polymer Science: Polymer Phys. Ed.*, **19** (1981) 1255-1267.
[2] Bruder F. and Brenn R., *Phys. Rev. Lett.*, **69** (1992) 624-627.

[3] Genzer J. and Kramer E. J., *Phys. Rev. Lett.*, **78** (1997) 4946-4949.
[4] Affrossman S., Henn G., O'Neill S. A., Pethrick R. A. and Stamm M., *Macromolecules*, **29** (1996) 5010-5016.
[5] Kumacheva E., Li L., Winnik M. A., Shinozaki D. M. and Cheng P. C., *Langmuir*, **13** (1997) 2483-2489.
[6] Krausch G., Kramer E. J., Rafailovich M. H. and Sokolov J., *Appl. Phys. Lett.*, **64** (1994) 2655-2657.
[7] Straub W., Bruder F., Brenn R., Krausch G., Bielefeldt H., Kirsch A., Marti O., Mlynek J. and Marko J. F., *Europhys. Lett.*, **29** (1995) 353-358.
[8] Tanaka K., Takahara A. and Kajiyama T., *Macromolecules*, **29** (1996) 3232-3239.
[9] Walheim S., Boltau M., Mlynek J., Krausch G. and Steiner U., *Macromolecules*, **30** (1997) 4995-5003.
[10] Karim A., Slawecki T. M., Kumar S. K., Douglas J. F., Satija S., Han C. C., Russell T. P., Liu Y., Overney R., Sokolov J. and Rafailovic M. H., *Macromolecules*, **31** (1998) 857-862.
[11] Henke B. L., Gullikson E. M. and Davis J. C., *At. Data Nucl. Data Tables*, **54** (1993) 181-342.
[12] Mark J. E., *Physical Properties of Polymers Handbook* (Woodbury, New York) 1996.
[13] Wagner A. J. and Yeomans J. M., *Phys. Rev. Lett.*, **80** (1998) 1429-1432.
[14] The simulations by Wagner and Yeoman assume a flat surface and only composition variations are simulated. We can only compare to their calculations in the early stages when the samples are still relatively flat and the morphology is essentially two-dimensional. Once the large spheres develop the surface tension and changes in viscosity become important, which has not been considered by Wagner and Yeoman.
[15] Jacobsen C., Williams S., Anderson E., Brown M. T., Buckley C. J., Kern D., Kirz J., Rivers M. and Zhang X., *Opt. Commun.*, **86** (1991) 351.
[16] Ade H., Zhang X., Cameron S., Costello C., Kirz J. and Williams S., *Science*, **258** (1992) 972.
[17] Zhang X., Ade H., Jacobsen C., Kirz J., Lindaas S., Williams S. and Wirick S., *Nucl. Instrum. Methods Phys. Res. A*, **347** (1994) 431-435.
[18] Zhang X., Balhorn R., Mazrimas J. and Kirz J., *J. Struc. Biol.*, **116** (1996) 335-344.
[19] It should be noted that the differences in surface friction and viscoelastic response are dependent on the driving frequency and hence cannot be used as absolute determinations of chemical composition.
[20] Capillary waves are also known to account for most of the roughness observed on the surface of molten polymer films (Zhao W. *et al.*, *Phys. Rev. Lett.*, **70** (1993) 1453).
[21] Zheng X., Rafailovich M. H., Sokolov J., Y S., Schwarz S. A., Sauer B. and Rubinstein M., *Phys. Rev. Lett.*, **79** (1997) 1453.
[22] Li Z., Tolan M., Hohr T., Kharas D., Qu S., Sokolov J., Rafailovich M. H., Lorenz H., Kotthaus J. P., Wang J., Sinha S. K. and Gibaud A., *Macromolecules*, **31** (1998) 1915-1920.
[23] From STXM imaging of the washed regions we were able to determine that even a small (approximately 20%) PMMA component prevents dissolution.
[24] A DI3000 AFM was used to create this image with an external modulation unit designed especially for these measurements. Since the polymer film is much larger in the lateral than in the normal direction, there is much less damping of a lateral alternating force field which enhances the image contrast.
[25] The actual angle of these features is rather shallow. Their appearance gets exaggerated by the display of the SFM data.
[26] The spikes right at the rim might be swelling artifacts of spikes that are right inside the rim or swollen encapsulated PS domains that have not yet merged with the large PS domains, and hence did not dissolve in the cyclohexane rinse. We have no real evidence from the NEXAFS data for PMMA spikes outside the PS domains. The amplitude of all features appear larger on the AFM scans than the STXM due to swelling of the PMMA in the cyclohexane washing process. The frequency of these spikes is less in the NEXAFS images than in the SFM images shown due to the longer annealing times for the sample imaged with NEXAFS.
[27] Anastasiadis S. H., Gancarz I. and Koberstein J., *Macromolecules*, **21** (1988) 2980.